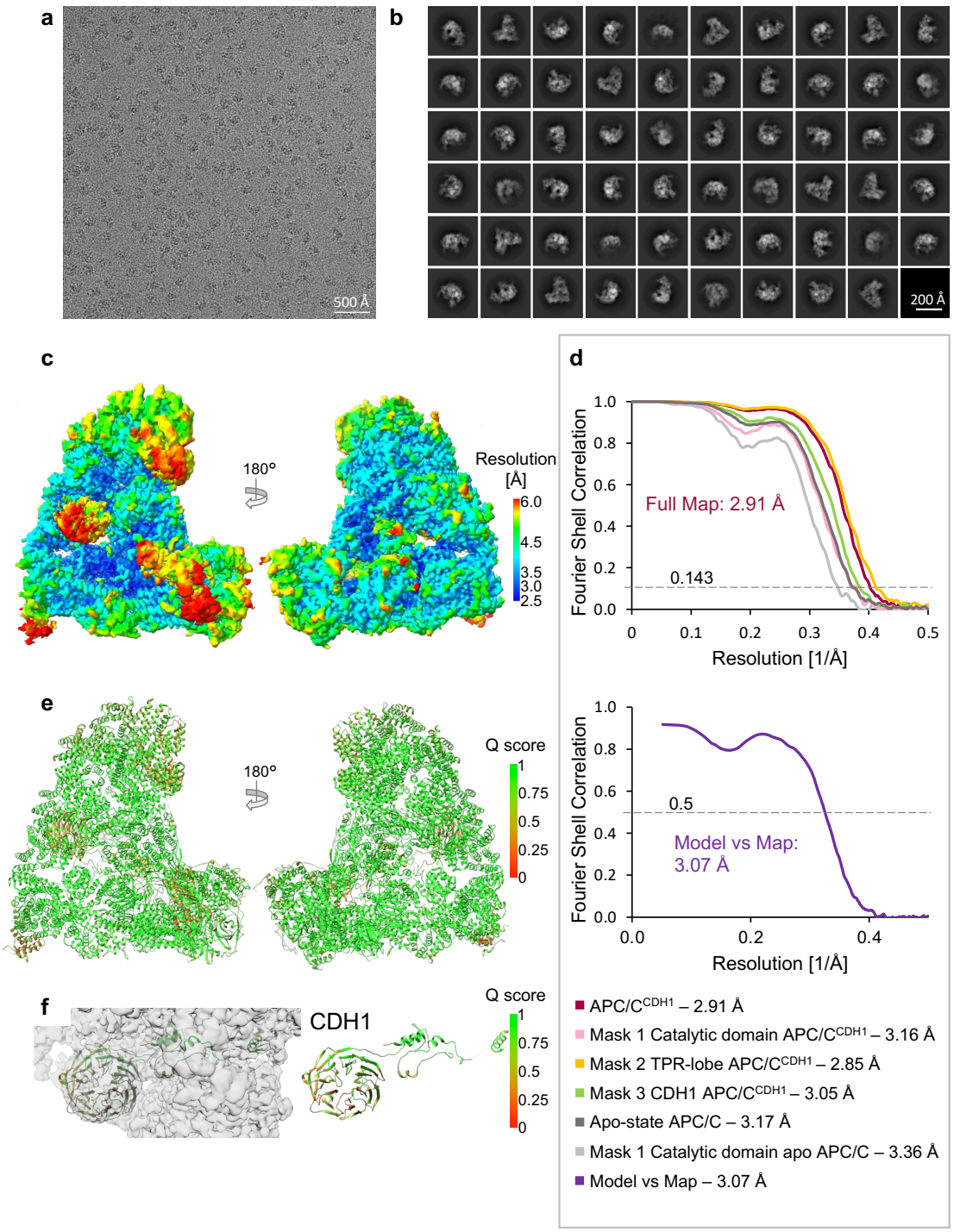

Supplementary Figure 1. Cryo-EM images and refined APC/C reconstructions. a, Representative cryo-EM image of the APC/C$^{CDH1:EMI1}$ complex. **b**, Gallery of 2D-class averages of APC/C$^{CDH1:EMI1}$. **c**, Local resolution map of APC/C$^{CDH1:EMI1}$. **d**, Fourier Shell Correlation (FSC) plots of the main maps used to generate molecular models. **e**, Q-score analysis [43] of the APC/C$^{CDH1:EMI1}$ complex to validate map-model correlation. **f**, Close-up view on the CDH1 subunit of the APC/C$^{CDH1:EMI1}$ complex that is colour-coded by Q-score.

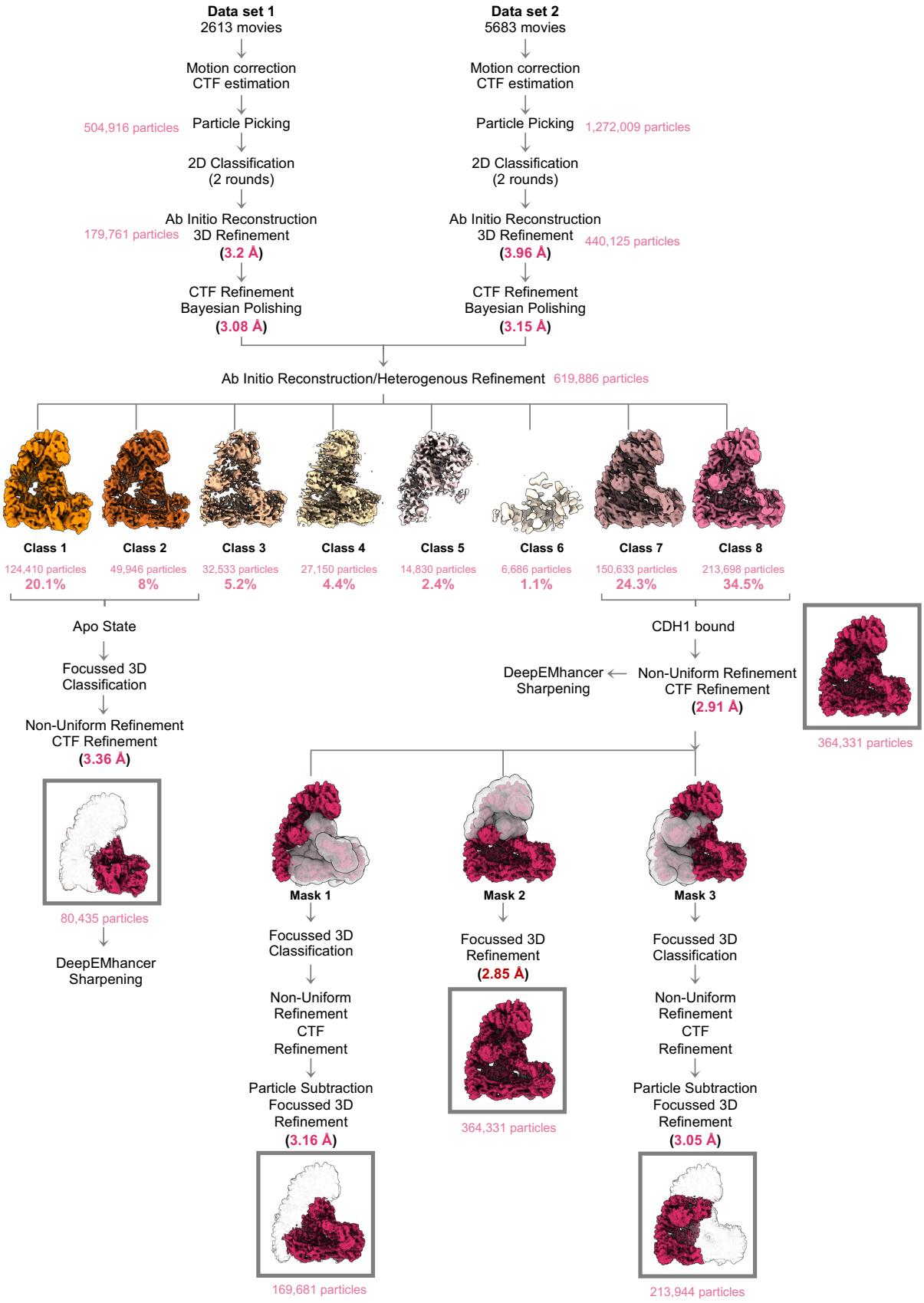

Supplementary Figure 2. Data processing pipeline for cryo-EM reconstructions. Cryo-EM data processing workflow summary as described in the Methods section.

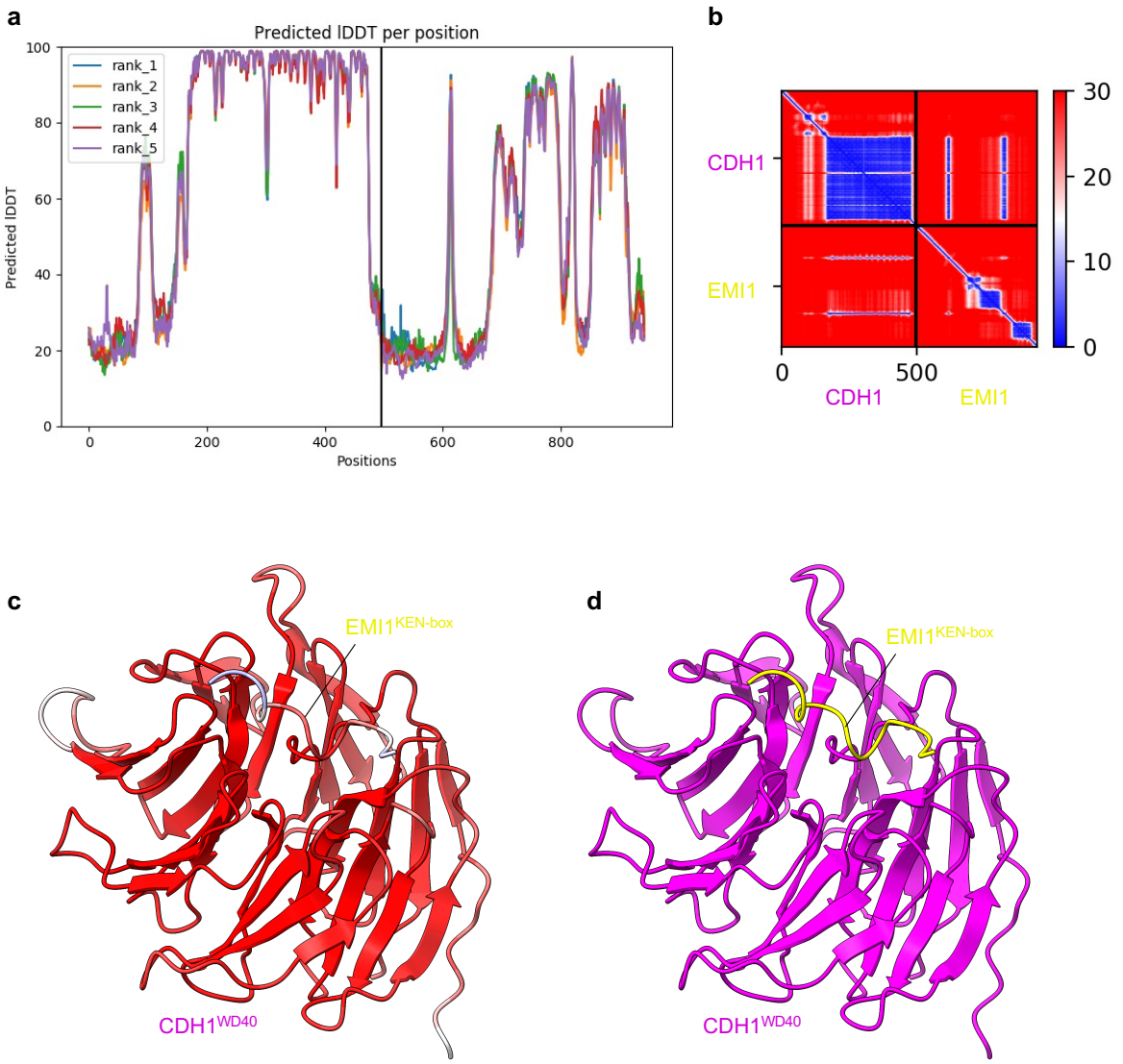

Supplementary Figure 3. AlphaFold2 prediction of the CDH1^{WD40}:EMI1$^{KEN\text{-}box}$ interaction and confidence metrics. **a**, Predicted local distance difference test (lDDT) values for the AlphaFold2 models of CDH1^{WD40}:EMI1$^{KEN\text{-}box}$. A higher score indicates higher confidence in the prediction. **b**, The predicted alignment error (PAE) heat map for the CDH1^{WD40}:EMI1$^{KEN\text{-}box}$ AlphaFold2 prediction. The PAE heat map shows the predicted error (in angstroms) between all pairs of residues, with blue indicating lower error and red indicating higher error. The PAE plot suggests high confidence for the predicted interactions between CDH1^{WD40} and EMI1$^{KEN\text{-}box}$. **c**, The pLDDT values mapped onto the predicted model of CDH1^{WD40}:EMI1$^{KEN\text{-}box}$. Residues are coloured in a scale of high (red) to low (blue) pLDDT values. The model was predicted with high confidence (pLDDT > 90). **d**, Predicted model colour-coded according to Fig. 1c.

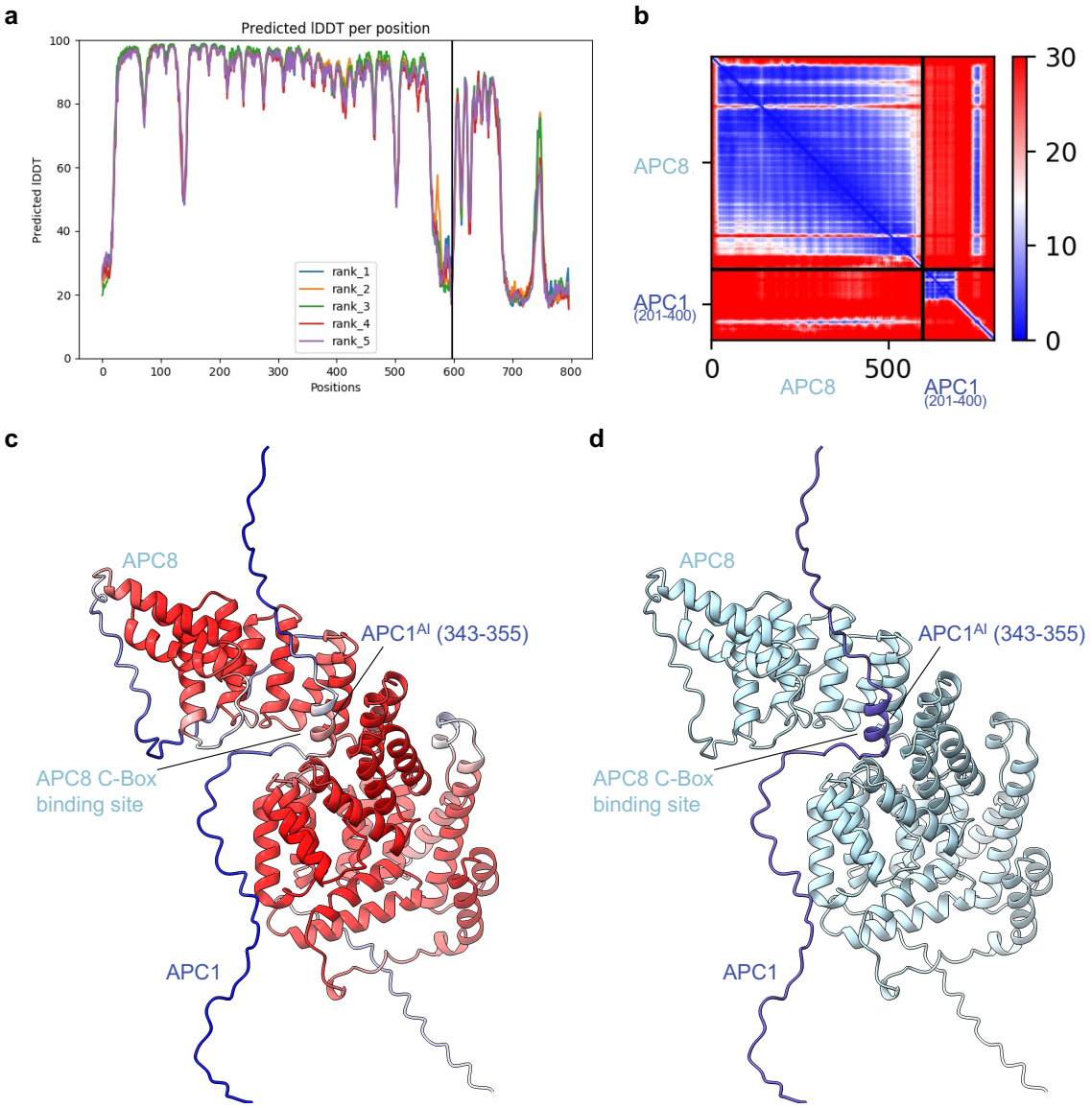

Supplementary Figure 4. AlphaFold2 prediction of the APC1^{AI}:APC8 interaction and confidence metrics. **a**, Predicted local distance difference test (lDDT) values for the AlphaFold2 models of APC1^{AI}:APC8. A higher score indicates higher confidence in the prediction. **b**, The predicted alignment error (PAE) heat map for the APC1^{AI}:APC8 AlphaFold2 prediction. The PAE heat map shows the predicted error (in angstroms) between all pairs of residues, with blue indicating lower error and red indicating higher error. The PAE plot suggests high confidence for the predicted interactions between APC1^{AI} and APC8. **c**, The pLDDT values mapped onto the predicted model of APC1^{AI}:APC8. Residues are coloured in a scale of high (red) to low (blue) pLDDT values. The model was predicted with high confidence (pLDDT > 90). **d**, Predicted model colour-coded according to Fig. 1c.

Supplementary Table 1. Cryo-EM data collection, refinement and validation statistics

	APC/C$^{CDH1:EMI1}$ Dataset 1		APC/C$^{CDH1:EMI1}$ Dataset 2		
Data collection					
Microscope	FEI Titan Krios		FEI Titan Krios		
Voltage (keV)	300		300		
Electron dose (e^-/Å^{-2})	40		40		
Detector	FEI Falcon III		FEI Falcon III		
Pixel size (Å/pixel)	1.07		1.07		
Defocus range (μm)	1.5-3.5		1.5-3.5		
Number of micrographs	2,613		5,683		
Reconstruction					
	APC/C^{apo}	APC/C$^{CDH1:EMI1}$	APC/C$^{CDH1:EMI1}$ Focussed Map Catalytic domain	APC/C$^{CDH1:EMI1}$ Focussed Map TPR lobe	APC/C$^{CDH1:EMI1}$ Focussed Map CDH1
Particles	174,356	364,331	169,681	364,331	213,944
Box size (pix)	360	360	360	360	360
Map sharpening B-factor (Å^2)	-116.8	-119.1	-106.3	-117.3	-121.3
Resolution (global, Å)	3.2	2.9	3.16	2.85	3.05
Resolution range(local, Å)	2.7-9.1	2.4-7.8	2.6-9.0	2.4-8.5	2.6-8.6
FSC threshold	0.143	0.143	0.143	0.143	0.143
Model composition					
Protein residues	8135	8926			
Ligands	1	6			
Refinement					
Resolution (Å)	3.4	3.1			
FSC threshold	0.5	0.5			
Model to map scores					
-CC	0.79	0.85			
B factors (Å^2)					
Protein residues	-83.2	-72.2			
Ligands	-106.9	-184.8			
R.m.s deviations					
Bond lengths (Å)	0.006	0.005			
Bong angles (°)	0.667	0.633			
Validation					
Clashscore, all atoms	11	10			
Rotamer outliers (%)	2.7	0.2			
Ramachandran plot					
Favoured (%)	97.26	95.86			
Allowed (%)	2.69	4.11			
Outliers (%)	0.05	0.02			
Deposition					
PDB ID	8PKP	7QE7			
EMDB ID	EMD-17751	EMD-13931			

Supplementary Table 2. Rebuilt regions of APC/C$^{CDH1:EMI1}$ subunits 7qe7

Subunit	Residue range	Modification	Comments	4ul9
APC1	135-145	Loop refitted		
	192-206	Loop refitted		
	275-283	Rebuild		
	282-295	α-helix to loop Helix now Cdh1^{N}		
	415-424	Loop fitted		
	460-464	Loop fitted		
	646-650	Loop rebuilt		
	671-681	α-helix built		
	701-734	Build (unassigned)		
	741-757	Build		
	814-838	Build		
	853-859	Build		
	882-901	Build		
	1009-1013	Build		
	1333-1347	Build		
	1433-1452	Build		
	1673-1684	Rebuild		
	1711-1734	Rebuild/build		
	1734-1911	Renumber -3		
	1825-1839	Build		
	1873-1877	Build		
	1897-1911	Build		
	1897-1936	Rebuild		
	1911-1935	Reverse chain polarity, fit s.c.		
APC2	16-35	s.c. built to α-helix		15-28, m.c. only
	46-52	Build		
	53-87	Rebuild and fit s.c.		
	126-147	Fit s.c.		Poly A
	187-233	Build/rebuild, fit s.c.	New Zn-binding module built: Cys 221,224, 231,233	
	304-322	Loop fitted		
	458-507	Rebuild		
	605-640		Good density	
	644-659		β-hairpin no density	
	660-720	m.c. good, s.c. poorly defined	Only poor part of APC2	
APC3 chain P	171-176	Build		
	177-445		Long disordered region	
	446-450	Build		
APC3 chain J	2-4	Build		
	171-176	Build		
	177-445		Long disordered region	
	446-450	Build		
	767-780	Rebuild		
APC4	126-133	Loop fitted		
	276-301	Rebuild		
	430-439	Loop fitted		

	465-470	Loop fitted		
	487-495	Rebuild		
APC5	9-27	Build		
	46-55	Rebuild		
	351-357	Rebuild		
	742-755	Rebuild		
APC6 chain K	94-98	Build		
	120-128	Build		
	544-567	Build: fit s.c. assigned to APC6		Poly A, unassigned chain
APC6 chain Q	No change			
APC7 chain Y	34-35	Build		
	553-555	Build		
APC7 chain Z	34-35	Build		
	131	Build		
	111-122	Build		
	371-540	Reposition α-helices		
APC8 chain V	499-509	Loop fitted		
APC8 chain U	499-509	Loop fitted		
	504-538	Rebuild		
	539-579	Build		
APC10	167-176	Rebuild, s.c. fitted		
APC11	1-8	Build β-strand		
	18-84	RING domain	m.c. and s.c.: good fit	
APC12 chain G	26-27	Build		
APC12 chain W	26	Build		
APC13	1-6	Rebuild		
	39-47	Build		
	68	Build		
APC15	No change			
APC16	51-57	Rebuild		
	108	Build		
CDH1	1-17	Build as α-helix		α-helix assigned to APC1 284-295
	40-42	Build		
	85-87	Build		
	109-125	Build		
	143-145	Build		
	164-172	Build	Connects to WD40	
	473-476	Rebuild		
EMI1	113-123	Build	KEN-box	
		RING domain 356-415	m.c. and s.c.: good fit	
	433-447	Fit s.c.	Incudes LRRL	

Supplementary Table 3. Summary of PIXE results

The number of atoms per molecule of all elements detected with a concentration greater than 3 x the limit of detection (LOD). Values quoted are the weighted mean of three-point analysis on a single protein spot for each sample.

Wild type APC2/APC11

Sulphur atoms per molecule: 48, used for internal normalisation to obtain Zn stoichiometry.

Weighted means	**P**	**Cl**	**Zn**
Atoms/mol (3)	2.95	1.52	**1.904**
LOD (atoms/mol)	0.643	0.335	**0.185**
Error (RSD %)	15.3	17	**13.4**

APC2/APC11 mutant protein

Sulphur atoms per molecule: 44, used for internal normalisation to obtain Zn stoichiometry.

Weighted means	**P**	**Cl**	**Zn**
Atoms/mol (3)	4.781	1.374	**0.957**
LOD (atoms/mol)	0.404	0.212	**0.11**
Error (RSD %)	10	12.3	**14.6**

Extended Data Table 4. Ordered and disordered regions of APC/C subunits

Subunit	Visible N-term	Visible C-term	Disordered regions	AF2 C-term helix	Protein Length (N)
APC1	10	1936	49-70, 197-202, 228-233, 285-398 (AI segment), 682-700, 735-740, 902-921, 988-1008, 1937-1944		1944
APC2	16	720	36-45, 491-495, 463-470, 721-822 (WH domain)		822
[1,2]APC3 chain P	5	769	177-445, 770-824, some density for 770-780 α-helix different orientation to P	783	824
[1,2]APC3 chain J	2	780	177-445, 781-824	783	824
APC4	3	758	127-133, 458-464, 759-808		808
APC5	9	755	21-24, 172-204 (linker), 454-456		755
[3]APC6 chain K	1	567	99-119 (AF2 α-helix 99-109), 529-543, 568-620	528	620
[3,4]APC6 chain Q	1	533	94-121 (AF2 α-helix 99-109), 534-630	528	620
APC7 chain Z	34	555	111-130, 556-565, AF2 α-helix 3-23 not visible	557	565
APC7 chain Y	35	540	113-130, 541-565, weak density for α-helix 542-555, AF2 α-helix 3-23 not visible	557	565
[5]APC8 chain V	24	557	558-597, some density for 568-579 segment	559	597
[5]APC8 chain U	24	579	136-144, 561-567, 580-597	559	597
APC10	3	185	None		185
APC11	1	84	None		84
APC12 chain G	1	27	28-85		85
APC12 chain W	1	26	27-85		85
APC13	1	68	69-74		74
APC15	2	57	58-121		121
APC16	51	108	1-50, 109-110		110
CDH1	1	496	18-39, 68-84, 133-142, 477-484		496
EMI1	320	447	1-319, 340-355, 421-432		447

Notes

[1]Different trajectory N-term of IR tail for CDH1 and APC10
[2]Residues 273-286 of APC3 insert predicted to bind IR-tail binding site of APC3, includes $T^{279}P$
[3]AF2: In free APC6, residues 596-620 of APC6 mimic residues 1-27 of APC12
[4]Residues 529-540 of APC6 chain Q interacts with APC8 chain U?
[5]AF2: Residues 587-C-term of APC8 binds to C-box/IR tail site of APC8

N-term and C-term residues of sequence